

This paper is published as part of a *Dalton Transactions* themed issue on:

Bioinspired Catalysis

Guest Editor Seiji Ogo
Kyushu University, Japan

Published in [issue 12, 2010](#) of *Dalton Transactions*

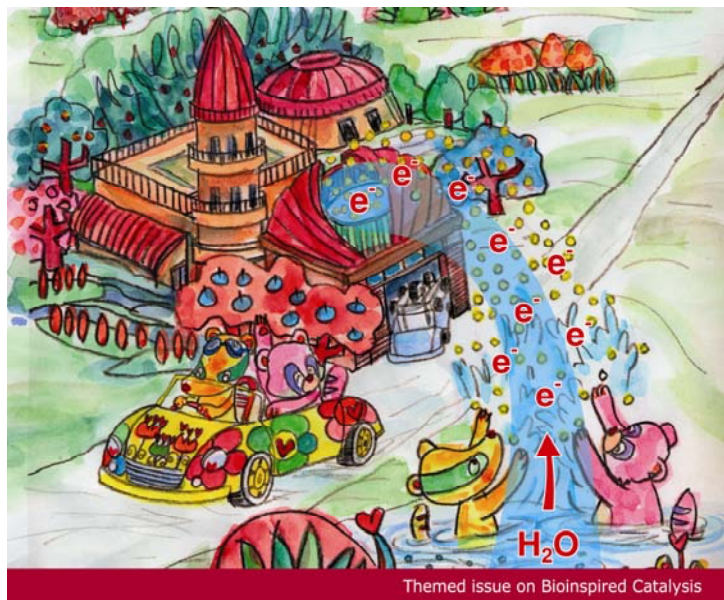


Image reproduced with permission of Seiji Ogo

Articles published in this issue include:

PERSPECTIVES:

[Mimicking Nitrogenase](#)

Ian Dance

Dalton Trans., 2010, DOI: 10.1039/b922606k

[Dual functions of NifEN: insights into the evolution and mechanism of nitrogenase](#)

Yilin Hu, Aaron W. Fay, Chi Chung Lee, Jared A. Wiig and Markus W. Ribbe

Dalton Trans., 2010, DOI: 10.1039/b922555b

[Quest for metal/NH bifunctional biomimetic catalysis in a dinuclear platform](#)

Takao Ikariya and Shigeki Kuwata

Dalton Trans., 2010, DOI: 10.1039/b927357c

COMMUNICATION:

[Chemiluminescence enhancement and energy transfer by the aluminium\(III\) complex of an amphiphilic/bipolar and cell-penetrating corrole](#)

Atif Mahammed and Zeev Gross

Dalton Trans., 2010, DOI: 10.1039/b916590h

Visit the *Dalton Transactions* website for more cutting-edge inorganic and bioinorganic research
www.rsc.org/dalton

Insertion reactions of CS₂, COS, and PhNCS at thiolate-bridged diiron centers†

Yanhui Chen, Ying Peng, Pingping Chen, Jinfeng Zhao, Litao Liu, Yang Li, Shuoyi Chen and Jingping Qu*

Received 30th September 2009, Accepted 16th November 2009

First published as an Advance Article on the web 23rd December 2009

DOI: 10.1039/b920144k

Treatment of [Cp*Fe(μ₂-SR)₃FeCp*] (**1a**, R = Et; **1b**, R = Me) with CS₂ obtains the insertion products [Cp*Fe(μ₂-SR)₂(μ-η²-S₂CSR)FeCp*] (**2a**, R = Et; **2b**, R = Me) with the retained Fe₂S₂ subunit in excellent yield. **2a** and **2b** represent the first examples for the CS₂ activation and incorporation at the diiron–SR bond. [Cp*Fe(μ₂-SEt)₂(μ-η²-S₂)FeCp*] (**3**) is prepared from COS and **1a** through the decarbonylation and sulfur coupling reaction of COS resulting in the formation of S₂²⁻ ligand. Addition of PhNCS into **1a** affords a mononuclear complex [Cp*Fe(SEt)(η²-SC(SEt)NPh)] (**4**). **1a** is found to be unreactive towards CO₂. The spectral characterization, X-ray diffraction analysis, and electrochemistry of the insertion products have also been described.

Introduction

The insertion of heterocumulenes including carbon dioxide (CO₂), carbon disulfide (CS₂), carbonyl sulfide (COS), and isothiocyanate (RNCS) into metal–non-metal bonds such as metal–hydride, metal–nitrogen, metal–oxygen, metal–carbon, and metal–sulfur bonds of transition metal fragments and their subsequent functionalization have drawn much attention due to their potential sources of C1 chemistry for the generation of useful organic compounds.^{1,2} The development of practical and effective methods for the transformations of these small molecules, especially CO₂, an abundant and inexpensive source of carbon, is essential for the future. Being structurally similar to CO₂, the diverse chemistry of CS₂ including coordination, addition, cleavage, and insertion reactions is currently being intensively investigated, as CS₂ is highly reactive and the transition metal complexes bearing CS₂ may be regarded as model compounds for CO₂ activation and transformation.³ Additionally, COS can function as a good carbonylating agent in the presence of a suitable thiophilic agent, and RNCS is useful as a source of carbon, nitrogen, and sulfur in one chemical step.^{4a}

Compared to the numerous insertion reactions with these small unsaturated molecules at the single transition metal center,^{4,9} an insertion at the di- or multi-metal centers has still remained poorly explored, and is just limited to several examples to get mononuclear insertion products: one is the insertion into nickel(II) hydroxido complexes,¹⁰ another one is about the reaction of Pt₂S(PPh₃)₃(CO) with CS₂ to get a mononuclear Pt complex (Ph₃P)₂PtS₂CS,¹¹ and the other two reactions are about C–S bond cleavage of CS₂ or PhNCS at the diiron centers and insertion of a S atom into the Fe=C or Fe–C bonds.¹² Another example is the insertion reactions of CO₂, Ph₂C=C=O and Me₃CNCO into Zr–

C bond of (η²-formaldehyde)zirconocene dimer affording mono- or di-insertion products in η¹ coordination mode.¹³ But to date, there is no example on the insertion reaction of CS₂, COS and PhNCS at the diiron–thiolate centers, although a lot of insertion reactions of heterocumulenes into M–SR bonds (M = Ru, Os, Pt, W, etc.)^{5b,6c–6e} at the single transition metal site have been reported.

Our group focuses on the synthesis and reactivity of diiron–sulfur clusters with Cp* as single ancillary ligands, which can provide bimetallic reaction sites and simulate biological metallo-proteins to activate small molecules. In our previous work, we have reported three new triply thiolate-bridged diiron complexes [Cp*Fe(μ₂-SR)₃FeCp*] (Cp* = η⁵-C₅Me₅; R = Me, Et, Ph) with excellent properties including the activation of C–Cl of some chlorohydrocarbons and the catalytic cleavage of N–N single bond of hydrazines under ambient conditions.¹⁴ As an extension of this work, herein we report the insertion reactions of [Cp*Fe(μ₂-SR)₃FeCp*] (**1a**, R = Et; **1b**, R = Me) with CS₂, COS, and PhNCS. The X-ray structures and characterizations of new complexes [Cp*Fe(μ₂-SR)₂(μ-η²-S₂CSR)FeCp*] (**2a**, R = Et; **2b**, R = Me), [Cp*Fe(μ₂-SEt)₂(μ-η²-S₂)FeCp*] (**3**), and [Cp*Fe(SEt)(η²-SC(SEt)NPh)] (**4**), together with the electrochemistry of **2a** and **2b**, are also discussed in this paper.

Results and discussion

As outlined in Scheme 1, reaction of [Cp*Fe(μ₂-SEt)₃FeCp*] (**1a**) with excess CS₂ at 40 °C affords complex [Cp*Fe(μ₂-SEt)₂(μ-η²-S₂CSEt)FeCp*] (**2a**) in excellent yield (100%) as a blue-purple microcrystalline powder. Complex [Cp*Fe(μ₂-SMe)₂(μ-η²-S₂CSMe)FeCp*] (**2b**) is also obtained in high yield (100%) in a similar way by treatment of [Cp*Fe(μ₂-SMe)₃FeCp*] (**1b**) with CS₂. Completely different from other insertion reactions on dinuclear transition metal complexes affording mononuclear products: [(N₃-mc2)Ni(S₂COR)](PF₆) (N₃-mc2 = 2, 4, 9-tetramethyl-1, 5, 9-triazacyclododec-1-ene, R = Me, Et)¹⁰ and (Ph₃P)₂PtS₂CS,¹¹ CS₂ molecule is incorporated into Fe–SR bond with binding to two Fe atoms and one SR ligand in **2a** and **2b**. Complexes **2a** and **2b** are paramagnetic at room temperature. The ¹H NMR spectrum of **2a** in C₆D₆ shows four broad signals at δ 1.44, 0.57, –0.79,

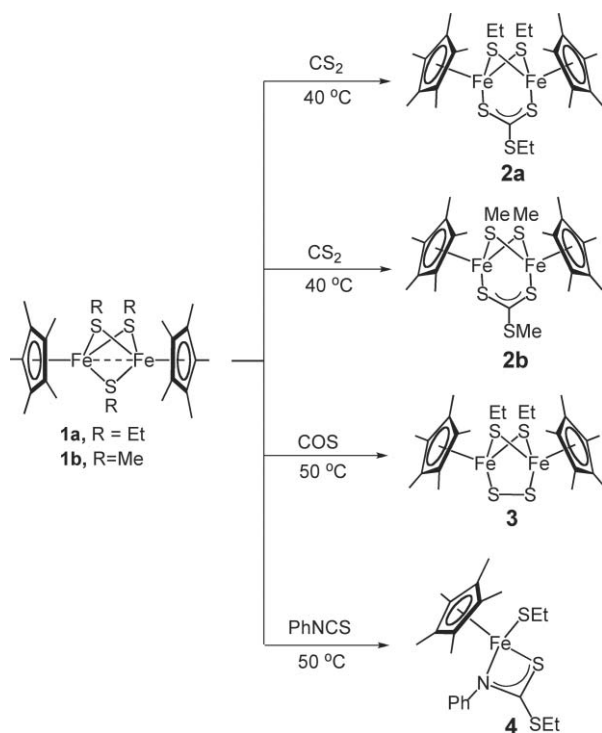
State Key Laboratory of Fine Chemicals, School of Chemical Engineering, Dalian University of Technology, Dalian, 116012, P. R. China. E-mail: Qujp@dut.edu.cn, Qujp@chem.dut.edu.cn; Fax: +86-411-8363-3080

† Electronic supplementary information (ESI) available: Selected bond distances and angles; cyclic voltammograms. CCDC reference numbers 737810 and 749168–749170 and 753805. For ESI and crystallographic data in CIF or other electronic format see DOI: 10.1039/b920144k

Table 1 Crystal data and structure refinement for complexes **2a**, **2b**, **3**, **4**

Complex Formula	2a C ₂₇ H ₄₅ Fe ₂ S ₅	2b C ₂₄ H ₃₉ Fe ₂ S ₅	3 C ₂₄ H ₄₀ Fe ₂ S ₄	4 C ₂₁ H ₃₀ FeNS ₃
Fw	641.63	599.55	568.50	448.49
T/K	293(2)	293(2)	293(2)	293(2)
Wavelength/Å	0.71073	0.71073	0.71073	0.71073
Crystal size/mm	0.33 × 0.32 × 0.28	0.35 × 0.33 × 0.25	0.43 × 0.31 × 0.26	0.16 × 0.13 × 0.11
Crystal system	Monoclinic	Monoclinic	Monoclinic	Monoclinic
Space group	P2 ₁ /n	C2/c	C2/c	P2 ₁ /c
a/Å	11.9506(2)	31.2295(12)	18.9893(6)	9.5932(15)
b/Å	15.2338(2)	11.3352(4)	12.8536(6)	15.484(2)
c/Å	16.6540(3)	16.2519(6)	11.2639(5)	15.385(2)
α/°	90	90	90	90
β/°	99.659(1)	97.191(2)	92.964(4)	90.014(12)
γ/°	90	90	90	90
V/Å ³	2988.93(8)	5707.8(4)	2745.6(2)	2285.4(6)
Z	4	8	4	4
ρ _c /g cm ⁻³	1.426	1.395	1.375	1.303
μ/mm ⁻¹	1.335	1.393	1.371	0.939
F(000)	1356	2520	1200	948
θ/°	2.29 to 27.50	1.91 to 25.00	2.60 to 24.98	1.87 to 25.00
Limiting indices	-15 ≤ h ≤ 15 -19 ≤ k ≤ 19 -21 ≤ l ≤ 21	-37 ≤ h ≤ 37 -13 ≤ k ≤ 12 -18 ≤ l ≤ 19	-22 ≤ h ≤ 21 -13 ≤ k ≤ 15 -13 ≤ l ≤ 12	-11 ≤ h ≤ 11 -15 ≤ k ≤ 18 -18 ≤ l ≤ 18
Refns collected	22845	22282	11074	12379
Refns unique	6380	5025	2420	4027
R _{int}	0.0290	0.0249	0.0236	0.0636
GOF(F ²)	1.034	1.079	1.062	1.026
R ₁ , ^a wR ₂ , ^b [I > 2σ(I)]	0.0346/0.0877	0.0325/0.0896	0.0270/0.0796	0.0595/0.1305
R ₁ , ^a wR ₂ , ^b (all data)	0.0429/0.0916	0.0393/0.0929	0.0321/0.0832	0.0803/0.1398
Largest diff. peak and hole/e Å ⁻³	0.518, -0.656	0.599, -0.407	0.231, -0.244	0.580, -0.280

$$^a R_1 = \sum \|F_o\| - |F_c| / \sum \|F_o\|, \quad ^b wR_2 = \{ \sum [w(F_o^2 - F_c^2)^2] / \sum [w(F_o^2)^2] \}^{1/2}.$$



Scheme 1 The insertion reactions of heterocumulenes at thiolate-bridged diiron centers.

-2.64, and -9.33 ppm assigned to the protons of CH₂ in S₂CSEt group, CH₂ in SEt, CH₃ in S₂CSEt, CH₃ in SEt, and the protons of two Cp* ligands, respectively. The ¹H NMR spectrum of **2b** exhibits three resonances at δ 12.44, -6.43, -8.84 ppm attributed to the protons of CH₃ in SMe group, CH₃ in S₂CSEt and CH₃ in two equivalent Cp* ligands, respectively. Both **2a** and **2b** are unambiguously characterized by single-crystal X-ray diffraction analysis, and their spectral features are fully consistent with their crystal structures. Crystallographic data are listed in Table 1.

Complex **2a** crystallizes in the monoclinic space group P2₁/n with four asymmetric molecules per unit cell. An ORTEP drawing of **2a** is shown in Fig. 1. The overall structure consists of two Cp*Fe units bridged by two *syn*-axial SEt ligands, in which the long Fe...Fe distance of 3.141(4) Å is indicative of the absence of a bonding interaction between the two Fe atoms.^{14a,15} The Fe₂S₂ ring is substantially puckered with a dihedral angle of 156° and two Cp* ligands are overlapped by each other along Fe1...Fe2 vector. The remaining sites of two Fe atoms are occupied by two S atoms from the S₂CSEt group resulting in the formation of tetrahedral coordination geometry of the iron center. There are no significant differences in the coordination geometry between two Fe atoms. Two Cp* ligands are in mutually *cis* orientation, and the dihedral angle between the Cp* rings in **2a** (62°) is apparently wider than that in the precursor **1a** (4.3°),^{14a} which may be a consequence of the incorporation of the larger S₂CSEt ligand in place of the SEt ligand. Fe1Fe2S3S4C25 are nearly coplanar with the deviation being 0.02°, whose dihedral angles with two Cp* rings are 90.3° and 86.9°, respectively. All the Fe-C bond

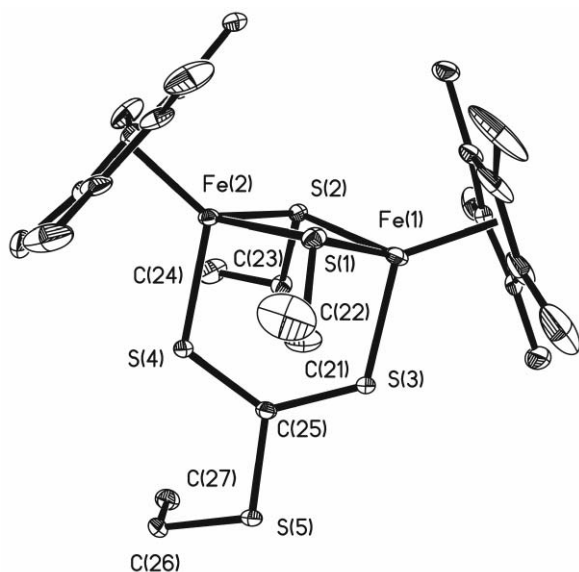


Fig. 1 Molecular structure of **2a**. Hydrogen atoms and one disordered SEt ligand are omitted for clarity (30% probability thermal ellipsoids). Selected bond lengths (Å) and angles (°): Fe(1)⋯Fe(2) 3.141(1), Fe(1)–S(1) 2.311(2), Fe(1)–S(2) 2.269(1), Fe(1)–S(3) 2.184(1), Fe(2)–S(1) 2.304(2), Fe(2)–S(2) 2.260(1), Fe(2)–S(4) 2.193(1), S(4)–C(25) 1.694(2), S(5)–C(25) 1.768(2), S(5)–C(26) 1.813(2), S(3)–C(25) 1.687(2), S(2)–Fe(1)–S(3) 97.0(1), S(2)–Fe(1)–S(1) 91.4(1), S(3)–Fe(1)–S(1) 92.1(1), S(4)–Fe(2)–S(2) 96.3(1), S(4)–Fe(2)–S(1) 92.4(1), S(2)–Fe(2)–S(1) 92.5(1), Fe(2)–S(2)–Fe(1) 87.8(1), Fe(2)–S(1)–Fe(1) 85.8(1), S(3)–C(25)–S(4) 129.3(1), S(3)–C(25)–S(5) 112.1(1), S(4)–C(25)–S(5) 118.8(1).

distances (2.101(3)–2.143(2) Å) fall in the normal range for Fe–C single bonds. The Fe–S (S atoms are from the SEt ligands) bond lengths (2.260(1)–2.311(1) Å) are obviously longer than those (2.184(1)–2.193(1) Å) of S atoms from the S₂CSEt group. In the S₂CSEt group, we can see that the S3–C25 and S4–C25 bond distances are almost equal (1.687(1), 1.694(1) Å), and are intermediate between single- and double-bond distances,¹⁶ which shows that the electrons are delocalized over the S–C–S unit.

Complex **2b** crystallizes in the monoclinic space group *C2/c* with eight asymmetric molecules per unit cell. The molecular structure of **2b** (Fig. 2) resembles that of **2a**. There is no interaction between the two Fe atoms (Fe⋯Fe distance: 3.350(1) Å). The dihedral angle between the two Cp* rings is 57° and smaller than that of **2a** (62°), while the dihedral angle of the butterfly-shaped Fe1S1Fe2S2 (34°) is significantly larger than that of **2a** (14°) along the Fe1⋯Fe2 vector. There is also an expected pattern of delocalization among S3, C23, and S4 atoms from the S₂CSEt ligand, where the S–C bond distances (1.704(3) Å, 1.677(3) Å) are comparable to those in **2a**, and shorter than the S5–C23 single bond (1.764(2) Å).

The formation of S₂CSR (R = Et, Me) in the insertion products **2a** and **2b** shows that the linear CS₂ molecule can be activated at the diiron centers. The process may be *via* the loss of the SR ligand and precoordination of CS₂ to the iron atoms,^{6b} followed by electrophilic attack through the CS₂ ligand on the sulfur atom of the thiolate ligand to get a S₂CSR (R = Et, Me) group as a consequence. Such coordination mode of a μ-η²-S₂CSR (R = Et, Me) group between two iron atoms represents a new type of heterocumulenes activation at the dinuclear metal centers.

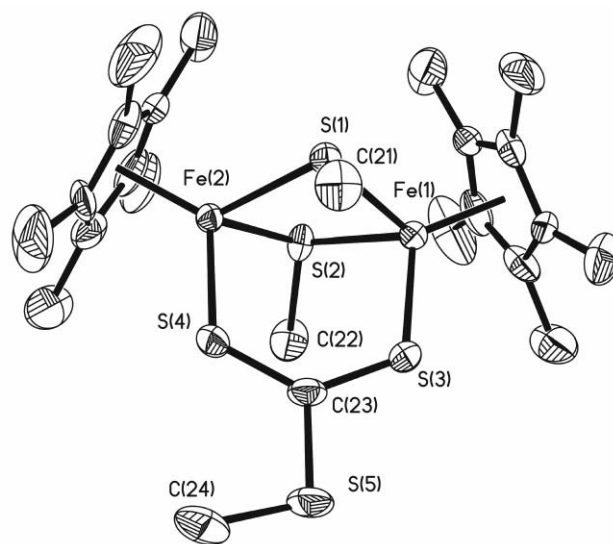


Fig. 2 Molecular structure of **2b**. Hydrogen atoms are omitted for clarity (30% probability thermal ellipsoids). Selected bond lengths (Å) and angles (°): Fe(1)⋯Fe(2) 3.350(1), Fe(1)–S(1) 2.273(1), Fe(1)–S(2) 2.253(1), Fe(1)–S(3) 2.179(1), Fe(2)–S(1) 2.264(1), Fe(2)–S(2) 2.255(1), Fe(2)–S(4) 2.162(1), S(3)–C(23) 1.704(3), S(4)–C(23) 1.677(3), S(5)–C(23) 1.764(2), S(3)–Fe(1)–S(2) 98.3(1), S(3)–Fe(1)–S(1) 99.0(1), S(2)–Fe(1)–S(1) 79.7(1), S(4)–Fe(2)–S(2) 97.9(1), S(4)–Fe(2)–S(1) 98.9(1), S(2)–Fe(2)–S(1) 79.9(1), Fe(2)–S(1)–Fe(1) 95.2(1), Fe(1)–S(2)–Fe(2) 96.0(1), S(4)–C(23)–S(3) 129.4(1), S(4)–C(23)–S(5) 119.5(1), S(3)–C(23)–S(5) 111.3(1).

Being structurally very similar to CS₂ and CO₂, the reaction of COS with the triply thiolate-bridged diiron complex **1a** is also investigated. Treatment of **1a** with 2.0 eq. COS in THF at 50 °C for 12 h affords complex [Cp*Fe(μ₂-SEt)₂(μ-η²-S₂)FeCp*] (**3**) as a red-brown crystalline solid in 37% yield (Scheme 1) and some unidentified complexes containing a CO ligand proved by IR. Complex **3** is diamagnetic at room temperature. The ¹H NMR spectrum of **3** exhibits a signal at 1.43 ppm corresponding to the protons of two Cp* ligands, and the resonances at 1.14 and 0.79 ppm are ascribed to the protons of CH₂ and CH₃ in SEt ligands. The molecular structure of **3** is confirmed by X-ray diffraction analysis, and its spectral features are fully in accordance with the crystal structure. **3** crystallizes in the monoclinic space group *C2/c* with eight asymmetric molecules per unit cell. As shown in Fig. 3, there is a planar Fe–S–S–Fe bridge and the ethyl sulfide ligands also bridge the two irons while each is bonded to a Cp* group. There is no metal–metal interaction between the two Fe atoms, and the Fe⋯Fe distance is 3.328(1) Å. The S–Fe–S angles vary between 77° and 94°. The dihedral angle of the two Cp* rings is 32°. The Fe–S bond distances (2.296(1), 2.135(1) Å) are in the normal range of Fe–S single bonds. The S–S bond distance in the S₂²⁻ ligand is 2.033(1) Å. All these structural parameters of **3** are comparable to the analogous diiron sulfur cluster [CpFe(μ₂-SEt)₂(μ-η²-S₂)FeCp] (Cp = C₅H₅) reported by L. W. Reeves and R. Rivest.¹⁷ Unlike the COS insertion into the Fe–H bond of monomer *cis*-Fe(dmpe)₂H₂ (dmpe = Me₂PCH₂CH₂PMe₂) yielding η¹-SCHO coordination to the Fe atom,^{5a} an unexpected bridging S₂²⁻ ligand is formed in **3**. Such formation shows that decarbonylation occurs when COS is inserted at the diiron centers, with the cleavage of the C–S bond from COS to get S and CO,

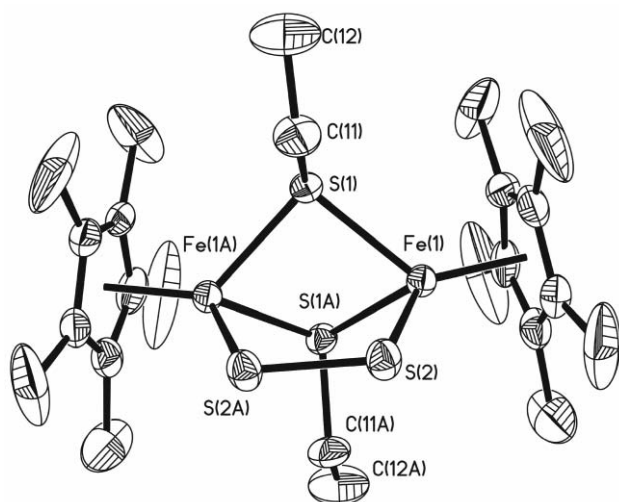


Fig. 3 Molecular structure of **3**. Hydrogen atoms and one disordered Cp* ligand attached to Fe1 atom are omitted for clarity (30% probability thermal ellipsoids). Selected bond lengths (Å) and angles (°): Fe(1)⋯Fe(1)^{#1} 3.328(1), Fe(1)–S(2) 2.135(1), S(1)–Fe(1)^{#1} 2.296(1), S(2)–S(2)^{#1} 2.033(1), S(2)–Fe(1)–S(1) 93.6(1), Fe(1)–S(1)–Fe(1)^{#1} 93.0(1), S(2)^{#1}–S(2)–Fe(1) 107.7(1), S(1)–Fe(1)–S(1)^{#1} 76.6(1).

and S atoms coupling to achieve S₂²⁻ ligand. This phenomenon also happens at a single metal center,^{1a} for example, the reaction between decamethylvanadocene and COS.¹⁸ The different reaction results of CS₂ and COS with **1a** reflects their distinct behaviors towards metal centers, although COS is structurally related to CS₂. Usually, the metal-(η²-CS₂) complexes are much more stable than the metal-(η²-COS) complexes, thus the elimination of sulfur from metal-(η²-CS₂) complexes is more difficult than metal-(η²-COS) complexes, as the weakening of the C=S bond of COS on coordination to a metal induced by dπ–π* back donation is apparently sufficient to promote the elimination of sulfur.

Treatment of **1a** with 2.0 eq. PhNCS in THF solution at 50 °C for 2 h produces complex [Cp*Fe(SEt)(η²-SC(SEt)NPh)] (**4**) as a red-brown crystalline solid in 46% yield (Scheme 1). Complex **4** is characterized by IR, ¹H NMR, elemental analyses and X-ray diffraction analysis. In the IR spectrum of **4**, the two strong absorptions at 1490 and 1025 cm⁻¹ can be assigned to the bidentate CN and CS vibrations in the SC(SEt)NPh ligand, respectively,¹⁹ which shows that this ligand is formed by the transfer of the SEt group to the PhNCS carbon atom. Complex **4** is diamagnetic at room temperature. The broad singlet at 7.34 ppm is attributed to Ph protons in the ¹H NMR of **4**, and the resonances at 6.24, 5.38, and 1.55 ppm correspond to the protons of CH₂, CH₃ in the SEt group, and Cp* ligand, respectively. The spectral features are fully consistent with its crystal structure. Complex **4** crystallizes in the monoclinic space group P2₁/c with four asymmetric molecules per unit cell. As shown in Fig. 4, complex **4** is a monomeric species in which the SC(SEt)NPh group is chelating to the four coordinated Fe atom in a η² arrangement. While in the incorporation of PhNCS into the Fe–H bonds of mononuclear complex *cis*-Fe(dmpe)₂H₂ (dmpe = Me₂PCH₂CH₂PMe₂),^{4a} η¹ S-bound SCHNPh ligands are observed in the insertion product *trans*-Fe(dmpe)₂(η¹-SCHNPh)₂. The Fe1–S3 bond distance (2.327(1) Å) in **4** is identical to the corresponding

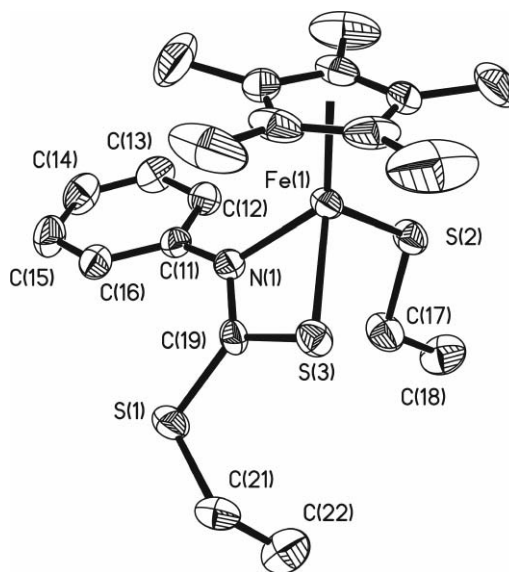


Fig. 4 Molecular structure of **4**. Hydrogen atoms are omitted for clarity (30% probability thermal ellipsoids). Selected bond lengths (Å) and angles (°): Fe(1)–N(1) 1.989(5), Fe(1)–S(2) 2.192(1), Fe(1)–S(3) 2.327(2), S(1)–C(19) 1.760(5), S(1)–C(21) 1.821(7), C(19)–N(1) 1.309(7), C(11)–N(1) 1.417(8), C(19)–S(3) 1.711(6), N(1)–Fe(1)–S(2) 96.4(1), N(1)–Fe(1)–S(3) 70.2(1), S(2)–Fe(1)–S(3) 99.3(1), C(19)–S(1)–C(21) 103.2(3), C(19)–S(3)–Fe(1) 77.8(2), N(1)–C(19)–S(3) 110.7(4), N(1)–C(19)–S(1) 124.5(4), S(3)–C(19)–S(1) 124.7(3), C(19)–N(1)–Fe(1) 101.0(4).

value (2.321(1) Å) in *trans*-Fe(dmpe)₂(η¹-SCHNPh)₂.^{4a} Similar to the CS₂ insertion of **2a** and **2b**, substantial electronic delocalization over the S–C–N unit is found, as the C19–S3 and C19–N1 bond lengths in complex **4**, 1.711(6) and 1.309(7) Å, are between the corresponding single and double bond distances.¹⁶

Electrochemistry

The cyclic voltammograms (CV) of **2a** and **2b** have been measured in THF–0.1 M [*n*-Bu₄N][PF₆]. The CV of **2a** shows three quasi-reversible redox peaks. The process observed at *E*_{1/2} = +0.37 V vs. Fc/Fc⁺ is assigned to [Fe^{II}Fe^{III}]/[Fe^{III}Fe^{III}],^{14a} one at *E*_{1/2} = –1.01 V is ascribed to [Fe^{II}Fe^{II}]/[Fe^{II}Fe^{III}], and another one at *E*_{1/2} = –1.92 V results from [Fe^IFe^{II}]/[Fe^{II}Fe^{II}].^{14a,20} In the case of **2b**, three quasi-reversible redox processes are also observed at *E*_{1/2} = +0.35, –0.97 and –1.90 V, which corresponds to [Fe^{III}Fe^{III}]/[Fe^{II}Fe^{III}], [Fe^{II}Fe^{II}]/[Fe^{II}Fe^{III}] and [Fe^IFe^{II}]/[Fe^{II}Fe^{II}], respectively. The quite close redox potentials of **2a** and **2b** indicate that SEt and SME ligands do not have a significant affect on the electrochemistry of the diiron complexes. Comparison to the electrochemistry of the precursor [Cp*Fe(μ₂-SMe)₂FeCp*] (**1b**) with the half-wave potential being 0, –0.95 and –1.98 V vs. Fc/Fc⁺ reflects a shift to a more positive potential in the process of [Fe^{II}Fe^{III}]/[Fe^{III}Fe^{III}] and two close redox potentials in the processes of [Fe^{II}Fe^{II}]/[Fe^{II}Fe^{III}] and [Fe^IFe^{II}]/[Fe^{II}Fe^{II}].

Conclusions

Thiolate-bridged diiron complexes [Cp*Fe(μ₂-SR)₂FeCp*] (**1a**, R = Et; **1b**, R = Me) react readily with small unsaturated molecules

CS₂, COS and PhNCS yielding insertion products [Cp*Fe(μ₂-SR)₂(μ-η²-S₂CSR)FeCp*] (**2a**, R = Et; **2b**, R = Me), [Cp*Fe(μ₂-SEt)₂(μ-η²-S₂)FeCp*] (**3**), and [Cp*Fe(SEt)(η²-SC(SEt)NPh)] (**4**). The heterocumulenes CS₂ and PhNCS are all bound to the metal iron atoms in a η² mode both in the dimer or monomer products. In the case of COS insertion reaction, decarbonylation and sulfur coupling reaction of COS happens at the diiron centers, obtaining S₂²⁻ ligand coordinating to the two Fe atoms also in η² fashion. **2a** and **2b** represent the first examples of CS₂ activation at thiolate-bridged diiron centers and insertion into the Fe-SR bond. These resulting insertion products may be regarded as model compounds for CO₂ activation and transformation at the di- or multi-metal centers.

Experimental

General procedures

All manipulations, unless otherwise stated, were carried out under an argon atmosphere using standard Schlenk-line techniques. All solvents were dried and distilled over an appropriate drying agent under argon. Complexes [Cp*Fe(μ₂-SEt)₂FeCp*] (**1a**)^{14a} and [Cp*Fe(μ₂-SMe)₂FeCp*] (**1b**)^{14b} were prepared according to the literature. CO₂, CS₂ and COS were commercially obtained and used as received. The ¹H NMR spectra were recorded on a Bruker 400 Ultra Shield spectrometer. Infrared spectra were measured on a NEXVSTM FT-IR spectrometer. Elemental analyses were performed on a Vario EL analyzer. Electrochemical measurements were recorded using a BAS-100W electrochemical potentiostat at a scan rate of 100 mV s⁻¹. Cyclic voltammogram was obtained in a three-electrode cell under argon in THF-0.1M [*n*-Bu₄N][PF₆]. The working electrode was a glassy carbon disk (diameter 3 mm), the reference electrode was a non-aqueous Ag/AgNO₃ electrode, and the auxiliary electrode was a platinum wire.

Syntheses

[Cp*Fe(μ₂-SEt)₂(μ-η²-S₂CSEt)FeCp*] (**2a**). 20 mL CS₂ was added to **1a** (0.45 g, 0.80 mmol) at ambient temperature, followed by refluxing for 2 h. The color of the solution turned from red-purple to blue-purple. The solvent was removed *in vacuo* and a blue-purple crystalline powder **2a** (0.51 g, 0.80 mmol, 100% yield) was obtained. The crystals of **2a** suitable for X-ray analysis were obtained by benzene solution layered with acetonitrile. **2a**: ¹H NMR (400 MHz, C₆D₆): δ 1.44 (br s, 2H, S₂CSCH₂CH₃), 0.57 (br s, 4H, SCH₂CH₃), -0.79 (br s, 3H, S₂CSCH₂CH₃), -2.64 (br s, 6H, SCH₂CH₃), -9.33 (br s, 30H, Cp*-CH₃). IR (KBr, cm⁻¹): 2964, 2899, 2860, 1447, 1427, 1371, 1253, 1157, 1069, 1020, 986, 900, 869, 755, 610, 453. Anal. Calcd for C₂₇H₄₅Fe₂S₅: C, 50.46; H, 7.21. Found: C, 50.42; H, 7.18.

[Cp*Fe(μ₂-SMe)₂(μ-η²-S₂CSMe)FeCp*] (**2b**). 20 mL CS₂ was added to **1b** (0.35 g, 0.68 mmol) at ambient temperature, followed by refluxing for 2 h. The color of the resulting solution turned from red-purple to blue-purple. The solvent was removed *in vacuo* and a blue-purple crystalline powder **2b** (0.40 g, 0.68 mmol, 100% yield) was isolated. The crystals of **2b** suitable for X-ray analysis were obtained by benzene solution layered with acetonitrile. **2b**: ¹H NMR (400 MHz, C₆D₆): δ 12.44 (br s, 6H, SCH₃), -6.43 (br s, 3H, S₂CSCH₃), -8.84 (br s, 30H, Cp*-CH₃). IR (KBr, cm⁻¹): 2963,

2901, 2867, 1426, 1370, 1308, 1289, 1261, 1097, 1019, 976, 945, 900, 844, 800, 685, 427. Anal. Calcd for C₂₄H₃₉Fe₂S₅: C, 48.00; H, 6.71. Found: C, 48.22; H, 6.78.

[Cp*Fe(μ₂-SEt)₂(μ-η²-S₂)FeCp*] (**3**). 2.0 eq. of COS (*ca.* 52 mL) was added by syringe to a solution of **1a** (0.65 g, 1.15 mmol) in 50 mL THF at room temperature. The resulting solution was heated to 50 °C and then stirred for 12 h with the color of solution changing from red-purple to red-brown. After removal of the solvent *in vacuo* the residue was purified by column chromatography on neutral alumina with n-hexane as the eluent to give **3** (0.23 g, 0.43 mmol, 37% yield) as a red-brown solid. The crystals of **3** suitable for X-ray analysis were obtained in concentrated n-hexane at -20 °C. **3**: ¹H NMR (400 MHz, C₆D₆): δ 1.43 (s, 30H, Cp*-CH₃), 1.14 (q, 4H, SCH₂CH₃), 0.79 (t, 6H, SCH₂CH₃). IR (KBr, cm⁻¹): 2963, 2907, 2867, 1474, 1447, 1426, 1373, 1261, 1097, 1021, 801. Anal. Calcd for C₂₂H₄₀Fe₂S₄: C, 48.89; H, 6.71. Found: C, 48.77; H, 6.68.

[Cp*Fe(SEt)(η²-SC(SEt)NPh)] (**4**). 2.0 eq. of PhNCS (0.29 g, 2.12 mmol) was added to a solution of **1a** (0.60 g, 1.06 mmol) in 30 mL THF at room temperature. The resulting solution was stirred for 2 h after it was warmed to 50 °C, and the color of solution turned from red-purple to red-brown. After removal of the solvent *in vacuo* the residue was purified by column chromatography on neutral alumina with n-hexane as the eluent to give red-brown solid **4** (0.44 g, 0.96 mmol, 46% yield). The crystals of **4** suitable for X-ray analysis were obtained in concentrated n-hexane at -20 °C. **4**: ¹H NMR (400 MHz, C₆D₆): δ 7.40 (br s, 5H, Ph), 6.24 (br s, 2H, SCH₂CH₃), 5.38 (br s, 3H, SCH₂CH₃), 1.25–2.52 (br s, 20H). IR (KBr, cm⁻¹): 3048, 2957, 2922, 2865, 1588, 1490, 1464, 1446, 1405, 1375, 1261, 1244, 1201, 1157, 1075, 1049, 1025, 983, 779, 707, 604, 497. Anal. Calcd for C₂₁H₃₀FeNS₃: C, 56.24; H, 6.74. Found: C, 56.27; H, 6.88.

X-Ray data collection and structure refinement

The data for complexes **2a**, **2b**, **3**, and **4** were collected on a Bruker SMART APEX CCD diffractometer with graphite monochromated Mo Kα radiation (λ = 0.71073 Å). Empirical absorption corrections were performed using the SADABS program.²¹ Structures were solved by direct methods and refined by full-matrix least-squares based on all data using F² using SHELX 97.²² All of the non-hydrogen atoms were refined with anisotropic thermal displacement coefficients. Hydrogen atoms were fitted geometrically at calculated distances and allowed to ride on the parent non-hydrogen atoms with the isotropic displacement being fixed at 1.2 and 1.5 times that of the aromatic and methyl carbon atoms that attached, respectively. For complex **2a**, the sulfur and carbon atoms of one thiolate ligand (S1C21C22) were refined disordered with the s.o.f. of the parts being refined using free variable, and thermal parameters on adjacent atoms in disordered moieties were restrained to be similar. For complex **3**, in order to assist the refinement, several restraints were applied: (1) the geometrical constraints of an idealized regular pentagon for one Cp* ligand bonding to an Fe1 center was used; (2) thermal parameters on adjacent carbon atoms in disordered moieties were restrained to be similar. In addition, the carbon atoms of this Cp* ligand attached to the Fe1 center were refined disordered with the s.o.f. of the parts being refined using free variable.

Acknowledgements

The authors thank the National Natural Science Foundation of China (No. 20972023, No. 20944003) and the Fund for Foreign Scholars in University Research and Teaching Programs of China for financial support of this work.

References

- (a) K. K. Pandey, *Coord. Chem. Rev.*, 1995, **140**, 37; (b) W. Leitner, *Coord. Chem. Rev.*, 1996, **153**, 257; (c) K. Tanaka, *Adv. Inorg. Chem.*, 1995, **43**, 409.
- G. Albertin, S. Antoniutti, E. Del Ministro and E. Bordignon, *J. Chem. Soc., Dalton Trans.*, 1994, 1769.
- (a) I. Omae, *Catal. Today*, 2006, **115**, 33; (b) R. Rossi, A. Marchi, A. Tiripicchio, *Organometallics*, 2007, **26**, 3840; (c) B. D. Ward, G. Orde, E. Clot, A. R. Cowley, L. H. Gade and P. Mountford, *Organometallics*, 2005, **24**, 2368; (d) H. Brombacher and H. Vahrenkamp, *Inorg. Chem.*, 2004, **43**, 6042; (e) E. Hevia, J. Pérez and V. Riera, *Organometallics*, 2003, **22**, 257; (f) A. Antiñolo, F. Carrillo-Hermosilla, S. Garcia-Yuste, M. Freitas, A. Otero, S. Prashar, E. Villaseñor and M. Fajardo, *Inorg. Chim. Acta*, 1997, **259**, 101.
- (a) L. D. Field, E. T. Lawrenz, W. J. Shaw and P. Turner, *Inorg. Chem.*, 2000, **39**, 5632; (b) M. Arroyo, S. Bernès, J. Cerón, J. Rius and H. Torrens, *Inorg. Chem.*, 2004, **43**, 986; (c) G. Albertin, S. Antoniutti and G. Roveda, *Inorg. Chim. Acta*, 2005, **358**, 3093.
- (a) V. Cadierno, M. P. Gamasa, J. Gimeno and E. Lastra, *J. Organomet. Chem.*, 1996, **510**, 207; (b) D. J. Darensbourg, B. L. Mueller, C. J. Bischoff, S. S. Chojnacki and J. H. Reibenspies, *Inorg. Chem.*, 1991, **30**, 2418; (c) A. Shaver, M. El-khateeb and A.-M. Lebuis, *Inorg. Chem.*, 2001, **40**, 5288; (d) A. Shaver, P.-Y. Plouffe, P. Bird and E. Livingstone, *Inorg. Chem.*, 1990, **29**, 1826; (e) I. Kovács and A. Shaver, *J. Organomet. Chem.*, 1999, **586**, 31.
- (a) J. Cámpora, E. Carmona, P. Palma and M. L. Poveda, *J. Chem. Soc., Perkin Trans. 1*, 1990, 180; (b) J.-F. Leboeuf, J.-C. Leblanc and C. Moïse, *J. Organomet. Chem.*, 1987, **335**, 331; (c) S. S. P. Almeida, M. T. Duarte, L. M. D. Ribeiro, F. Gormley, A. M. Galvão, J. J. R. Fraústo Da Silva and A. J. L. Pombeiro, *J. Organomet. Chem.*, 1996, **524**, 63.
- (a) O. R. Allen, S. J. Dalgarno, L. D. Field, P. Jensen and A. C. Willis, *Organometallics*, 2009, **28**, 2385; (b) E. B. Brouwer, P. Legzdins, S. J. Rettig and K. J. Ross, *Organometallics*, 1993, **12**, 4234; (c) P. Mathur, A. K. Ghosh, S. Mukhopadhyay, C. Srinivasu and S. M. Mobin, *J. Organomet. Chem.*, 2003, **678**, 142.
- (a) T. Gandhi, M. Nethaji and B. R. Jagirdar, *Inorg. Chem.*, 2003, **42**, 4798; (b) T. Gandhi, M. Nethaji and B. R. Jagirdar, *Inorg. Chem.*, 2003, **42**, 667; (c) T. Gandhi and B. R. Jagirdar, *Inorg. Chem.*, 2005, **44**, 1118.
- M. D. Santana, M. Sáez-Ayala, L. García, J. Pérez and G. García, *Eur. J. Inorg. Chem.*, 2007, 4628.
- C. T. Hunt, G. B. Matson and A. L. Balch, *Inorg. Chem.*, 1981, **20**, 2270.
- (a) G. Hogarth, M. H. Lavender and K. Shukri, *J. Organomet. Chem.*, 2000, **595**, 134; (b) V. Crocq, J.-C. Daran and Y. Jeannin, *Organometallics*, 1991, **10**, 448.
- G. Erker, M. Mena, S. Werner and C. Krüger, *J. Organomet. Chem.*, 1990, **390**, 323.
- (a) Y.-H. Chen, Y.-H. Zhou and J.-P. Qu, *Organometallics*, 2008, **27**, 666; (b) Y.-H. Chen, Y.-H. Zhou, P.-P. Chen, Y.-S. Tao, Y. Li and J.-P. Qu, *J. Am. Chem. Soc.*, 2008, **130**, 15250.
- P. D. Frisch, M. K. Lloyd, J. A. McCleverty and D. Seddon, *J. Chem. Soc., Dalton Trans.*, 1973, 2268.
- G. Häfelfinger, *Chem. Ber.*, 1970, **103**, 2902.
- (a) A. Terzis and R. Rivest, *Inorg. Chem.*, 1973, **12**, 2132; (b) G. T. Kubas, T. G. Spiro and A. Terzis, *J. Am. Chem. Soc.*, 1973, **95**, 273.
- S. Gamarotta, M. L. Fiallo, C. Floriani, A. C. Villa and C. Guastini, *Inorg. Chem.*, 1984, **23**, 3532.
- (a) U. Segerer, J. Sieler and E. Hey-Hawkins, *Organometallics*, 2000, **19**, 2445; (b) M. Wang, S.-W. Lu, M.-Z. Bei, H.-F. Guo and Z.-S. Jin, *J. Organomet. Chem.*, 1993, **447**, 227.
- (a) S. Dev, Y. Mizobe and M. Hidai, *Inorg. Chem.*, 1990, **29**, 4797; (b) C. Zimmermann, C. E. Anson, A. L. Eckermann, M. Wunder, G. Fischer, L. Keilhauer, E. Herrling, B. Pilawa, O. Hampe, F. Weigend and S. Dehnen, *Inorg. Chem.*, 2004, **43**, 4595; (c) T. Toan, B. K. Teo, J. A. Ferguson, T. J. Meyer and L. F. Dahl, *J. Am. Chem. Soc.*, 1977, **99**, 408.
- G. M. Sheldrick, *SADABS, Program for area detector adsorption correction*, Institute for Inorganic Chemistry, University of Göttingen, Germany, 1996.
- (a) G. M. Sheldrick, *SHELXL-97, Program for refinement of crystal structures*, University of Göttingen, Germany, 1997; (b) G. M. Sheldrick, *SHELXS-97, Program for solution of crystal structures*, University of Göttingen, Germany, 1997.